Available online at www.sciencedirect.com
SCIENCE DIRECT®
Journal of Nuclear Materials 336 (2005) 120–124
journal of nuclear materials
www.elsevier.com/locate/jnucmat

Surface modification of Hastelloy C-276 by SiC addition and electron beam melting

M. Ahmad [a], J.I. Akhter [a,*], M. Iqbal [a], M. Akhtar [a], E. Ahmed [a], M.A. Shaikh [a], K. Saeed [b]

[a] Physics Research Division, Pakistan Institute of Nuclear Science and Technology, P.O. Nilore, Islamabad, Pakistan
[b] Nuclear Materials Division, Pakistan Institute of Nuclear Science and Technology, P.O. Nilore, Islamabad, Pakistan

Received 3 June 2004; accepted 17 September 2004

Abstract

Electron beam surface melting of Hastelloy C-276 with the SiC addition is carried out to improve the surface properties. The resulted microstructure and non-equilibrium phases are characterized by X-ray diffraction (XRD), scanning electron microscopy (SEM) and energy dispersive system (EDS). The Hastelloy C-276 is successfully surface-hardened by electron beam melting, the surface hardening effect can be attributed to both microstructure refinement and eutectic phases produced by EB. During EB melting the SiC broke into small pieces and spread in the microstructure increasing the surface hardness by thirteen times.

1. Introduction

Electron beam surface melting is known to be a superior technique to refine the microstructure of alloy surfaces. It also offers a high degree of flexibility of heat source. Electron beam guns are high-temperature heat sources, which are able to melt and even, can evaporate all types of materials under the beam spot. As the spot size of the electron beam is very small, the cooling rate of the localized melt is very high. Rapid solidification is a field of considerable interest for both applied and fundamental research due to a variety of reasons discussed in the literature [1–10]. For example, the grain refinement of the melt during solidification can be achieved when a material is undercooled beyond a critical undercooling temperature. The rapid cooling of the melt leads to a significant deviation from local equilibrium at the solid–liquid interface which not only affects the solute trapping across the interface but also affects the diffusion temperature field around the interface and the kinetics of the crystal growth, which in turn influences the solidification mechanism.

Hastelloy C-276 is a Ni-base superalloy used in nuclear, chemical and aerospace industries due to its high corrosion resistance and high strength at elevated temperature. There are certain components, such as agitator blades, in the nuclear industry where both wear and corrosion resistance are required. Previous investigations on Hastelloy C-276 [11,12] indicated that ageing heat treatments increased the hardness of the alloy. The hardness of the alloy was found to increase due to the formation of P, M_6C and μ phases. The P and μ phases

* Corresponding author. Tel.: +92 51 2207224; fax: +92 51 9290275.
E-mail addresses: jiakhter@yahoo.com, akhterji@pinstech.org.pk, maqomer@yahoo.com (J.I. Akhter).

0022-3115/$ - see front matter © 2004 Elsevier B.V. All rights reserved.
doi:10.1016/j.jnucmat.2004.09.010

are deleterious in nature. The hard and brittle nature of the μ phase produced in Hastelloy C-276 during ageing has also been reported [13,14].

It is well established that laser or electron beam surface melting techniques can increase the microhardness of surfaces. In order to withstand high stresses in general engineering components such as bearings and gears, deep case hardening is often required. Electron beam melting provides the deep case hardening as compared to the laser melting. Dong et al. [15] studied the microstructure and hardness of the Ti–8.5%Si alloy surface melted by EB. Their observations showed that the hardness of the EB-molten surface was about 40–50% higher than the original surface. They attributed the surface hardening to the higher content of Si in the solid solution and the resulting fine microstructure. Bruckner et al. [16] succeeded in enhancing the surface hardness and tensile strength of EB-molten surface of $AlSi_{12}$ alloy about 50% and 60%, respectively, compared to the bulk alloy.

The addition of SiC in alloys produces composite structures with improved mechanical properties and in general without degrading corrosion resistance. However, wetting is always a problem in conventional melting. EB melting could overcome this problem as local melting occurs. There is no report available in the literature on the surface hardening of Hastelloy C-276 by EB surface melting technique. The surface melting of Hastelloy C-276 with the addition of SiC is carried out to achieve the composite structure at the surface with improved hardness and wear resistance. Microhardness and microstructural studies are performed to investigate the effect of EB surface melting in the presence of SiC particles.

2. Experimental

The nominal composition of the Hastelloy C-276 is given in Table 1. Samples of the size $10 \times 20 \times 3\,mm^3$ were cut from the sheet. Grids of the size $2 \times 3\,mm^2$ having a depth about 1 mm were made on the surface of the alloy C-276 by a spark erosion machine. SiC (called primary SiC in the subsequent discussion) was pressed into the grids, made on the surface of the alloy, by hydraulic press using a pressure of 4.9 kbar. An electron beam, with its direction normal to the surface, was used to melt the surface of the alloy. The parameters used for surface melting were, voltage = 40 kV, beam current = 12 mA, beam travel speed = 100 mm/s, and the beam was used in vibrational mode. The samples were kept in contact with a Cu mold of size $5 \times 6\,cm^2$ during melting to achieve a higher cooling rate. In order to reveal the microstructure, the surfaces were polished on a lapping machine up to 0.25 μm and immersed for two minutes in a solution of 80 ml HCl, 4 ml HNO_3, 1 g $CuCl_2$ and 20 ml glycerin.

Microstructural investigations were carried out using scanning electron microscopy (SEM) having the attachment of an energy dispersive system (EDS). Quantitative analysis was done using the Ni, Cr, Fe and Co Kα lines, the Mo Lα line and W Mα line and a ZAF correction procedure. Microhardness measurements were done using the load of 1.96 N. The phases were also characterized by XRD using the Cu $K\alpha_1$ line with $\lambda = 154.051$ pm radiation.

3. Results and discussion

3.1. Microstructure

The microstructure of as-received Hastelloy C-276 is shown in Fig. 1, which consists of equiaxed grains of the size ranging from 100 to 200 μm. Fig. 2 shows the microstructure of the EB-molten surface containing SiC and it looks completely different from the as-received alloy. The microstructure of the molten surface consists of dendrites in a eutectic matrix. EDS spectra of the dendritic phase and the eutectic phase are shown in Fig. 3. The composition of the dendrites and the eutectic matrix is given in Table 1. These dendrites are found to be depleted in Mo and Cr and rich in Ni and Fe while the eutectic matrix is enriched in Mo, Cr and W. The size of the dendrite along the the horizontal surface is large as compared to the vertical. The size of the dendrites

Table 1
Composition (in wt%) of as-received alloy and phases in the EB-molten zone

Element	As-received alloy	Dendrite (black contrast phase) (Cr–Mo depleted phase (α-Ni))	Eutectic Mo–Cr–W-rich phase (MoNi + solid solution)	Gray contrast layer around SiC
Cr	15.71	11.86	20.79	22.21
Fe	5.38	6.70	3.31	2.36
Co	1.59	1.86	1.3	1.49
Ni	54.91	64.34	28.68	41.63
Mo	17.32	8.9	33.67	5.17
W	5.09	6.35	12.25	0.19
Si	–	–	–	26.96

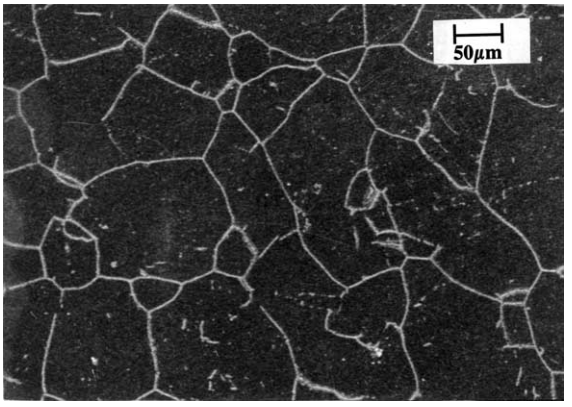

Fig. 1. SEM micrograph showing the microstructure of as-received Hastelloy C-276.

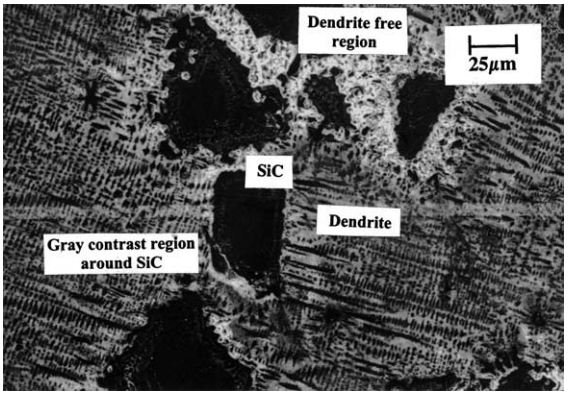

Fig. 2. SEM micrograph showing the microstructure of EB-molten surface of Hastelloy C-276. The direction of the EB is normal to the surface.

on the surface normal to the movement of the beam varies from 2 to 10 μm and the size along the beam travel direction is 0.7–3.0 μm. The microstructure of the eutectic phase is very fine and is shown in Fig. 4. The space between the stripes is less than 100 nm. The small space between the stripes is due to the higher cooling rate achieved by high melting speed and high conduction of heat through the Cu mold.

The primary SiC added at the surface was of average size around 70 μm. Fig. 5 shows the microstructure of the region with primary SiC along with secondary SiC particles present in a eutectic matrix around the primary SiC. The presence of secondary SiC particles around the primary SiC indicates that primary SiC has broken from the edges into secondary particles during the electron beam interaction and these carbide particles may act as a conducting source of heat during melting of the surface, and the melt around these particles cools slowly as compared to area without SiC. This eutectic matrix

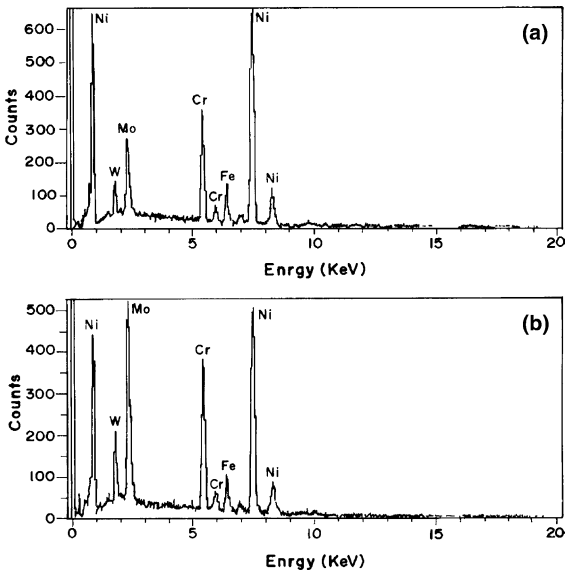

Fig. 3. EDS spectra of (a) dendritic phase and (b) eutectic phase.

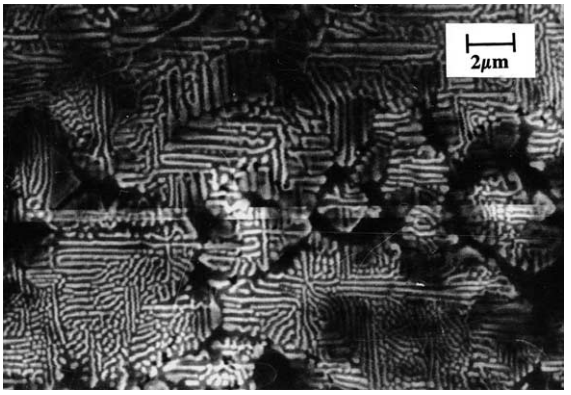

Fig. 4. Microstructure of the eutectic phase.

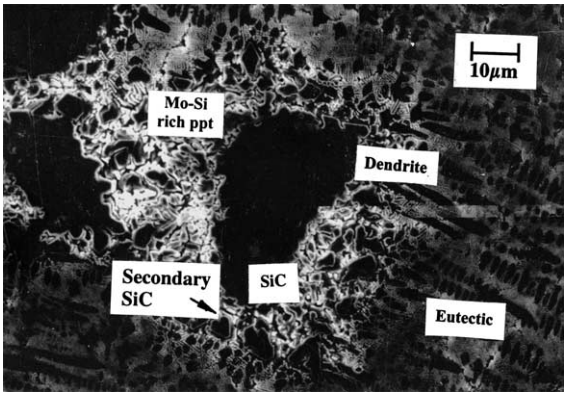

Fig. 5. SEM micrograph showing the microstructure of the region containing secondary SiC around the primary SiC.

having secondary SiC is rich in Mo, Cr, W and Si. However, Mo and Cr depleted dendrites are not observed in these regions. The eutectic matrix of this region also contains small amounts of Si diffused from broken SiC due to their interaction in the melt. The microstructure of the eutectic phase in this area is coarse as compared to the regions without secondary SiC. The space between the stripes of this region is 100–150 nm. Some primary SiC particles showing grey contrast at the edges are also shown in Fig. 2. The composition of grey contrast regions of this SiC is also given in Table 1. The grey contrast seems to be produced due to the Ni and Cr diffusion at the edges.

3.2. X-ray diffraction

X-ray diffraction (XRD) pattern of the as-received alloy and the molten surface containing SiC are shown in Fig. 6. The X-ray diffraction data analysis of the EB-molten surface and as-received alloy is given in Table 2. XRD patterns and analysis of the EB-molten surface indicate the presence of another phase, which is identified as MoNi along with the Hastelloy C-276 peaks. Peaks marked as (▲) in the EB-molten sample are the same as in the as-received samples but the peaks marked as (■) belong to the MoNi phase (eutectic phase). The difference in intensities between the peaks marked as (▲) in the EB-molten surface and the as-received alloy is due to the appearance of the new phase

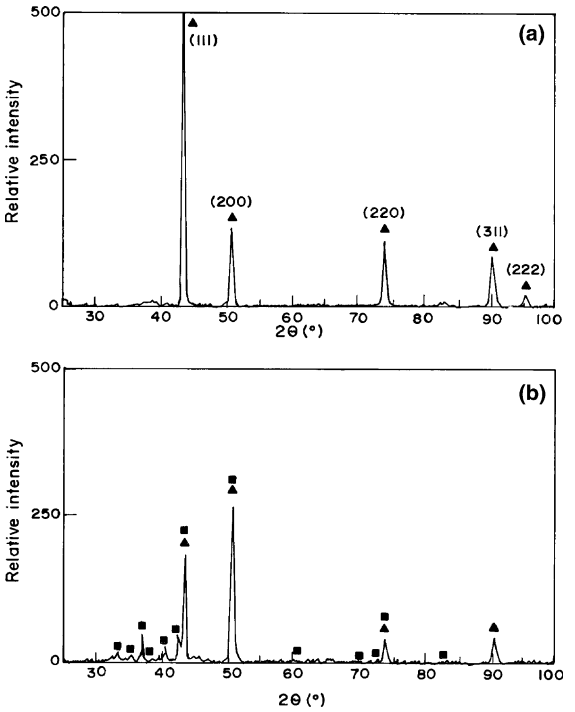

Fig. 6. XRD patterns of (a) as-received and (b) EB-molten surface of Hastelloy C-276. The symbols ▲ and ■ represent the peaks from the as-received sample and eutectic MoNi phase, respectively.

Table 2
XRD analysis of EB-molten surface of Hastelloy C-276 and as-received alloy

EB-molten surface					Identification of phases	As-received Hastelloy C-276				
Lattice spacing (nm)	h	k	l	I/I_0		Lattice spacing (nm)	h	k	l	I/I_0
0.2758	1	3	1	3	MoNi	0.2089	1	1	1	100
0.2687	1	1	3	6	MoNi	0.181	2	0	0	27
0.2534	3	2	0	4	MoNi	0.1278	2	2	0	23
0.242	1	3	2	19	MoNi	0.1089	3	1	1	17
0.2224	0	4	1	11	MoNi	0.1043	2	2	2	5
0.2113	3	0	3	16	MoNi					
0.208	1	1	1	67	Hastelloy C-276					
	3	3	1		MoNi					
0.1993	2	4	1	4	MoNi					
0.1943	2	3	3	3	MoNi					
0.1804	2	0	0	99	Hastelloy C-276					
	0	4	3		MoNi					
0.1525	1	5	3	2	MoNi					
0.1489	3	5	2	3	MoNi					
0.1438	2	3	5	2	MoNi					
0.1424	5	4	0	3	MoNi					
0.1352	5	4	2	2	MoNi					
0.1275	2	2	0	17	Hastelloy C-276					
	0	5	5		MoNi					
0.1293	0	7	1		MoNi					
0.1086	3	1	1	18	Hastelloy C-276					

Table 3
Microhardness of as-received alloy and different regions of the modified surface

Region	As-received	Eutectic phase	Secondary SiC + eutectic
Hardness (HV)	152 ± 10	550 ± 10	1987 ± 10

on the surface which was introduced during surface melting and fast cooling.

The dendrite structure rich in Ni, Fe and depleted in Cr, Mo have nucleated during the rapid solidification of the molten zone. Remaining liquid became rich in Mo, Cr and W due to the rejection of these elements in the liquid phase during the solidification giving rise to eutectic phase frozen with higher contents of Mo, Cr and W. The higher concentrations of Mo, Cr and W were also observed in the eutectic by EDS. This phase was confirmed by EDS and XRD as MoNi + solid solution. The dendritic phase rich in Ni and Fe and the SiC phase observed by SEM/ EDS were not detected by XRD, the reason may be that the volume density of these phases is very low compared to other phases.

3.3. Hardness

The microhardness is measured and average values of minimum five measurements along with errors for different areas are given in Table 3. The microhardness of the molten surface is HV 550. This higher hardness is due to the presence of higher Mo, Cr and W contents in the eutectic phase and the development of very fine microstructure due to the fast cooling rate. The presence of the dendritic phase also acts as a barrier against the movement of dislocations.

An increase of about thirteen times in hardness was achieved in the region containing secondary SiC particles spread in the fine eutectic matrix having small Si content, around the secondary SiC particles. This secondary SiC acts as a dispersoid and hinders the movement of the dislocations thus resulting in an increase of the hardness on the surface of this region. Another factor in increasing the hardness of this region is the introduction of Si into the crystal lattice. It is reported that Si is a very powerful solid solution strengthening agent [17].

4. Conclusions

1. The hardness of the EB-molten surface increased by four times due to the fine eutectic microstructure and the dendrites.
2. The primary SiC breaks into secondary SiC under the electron beam and spreads in the melt around the primary SiC.
3. The increase of hardness in the region containing secondary SiC increased by thirteen times compared to the original surface hardness of the alloy.

Acknowledgments

The authors are very thankful to Mr Shaker, Principal Engineer of the workshop for helping in EB surface melting of the samples. We are also grateful to the staff members of the Radiation Damage Group, PRD for assistance during the experimental phase of this work.

References

[1] S.L. Sobolev, Phys. Rev. E 55 (1997) 6845.
[2] M.J. Aziz, T. Kaplan, Acta Metall. 36 (1988) 2335.
[3] W.W. Mullins, R.F. Sekerka, J. Appl. Phys. 35 (1964) 444.
[4] K. Eckler, D.M. Herlach, M.J. Aziz, Acta Metall. Mater. 42 (1994) 975.
[5] S.J. Cook, P. Clancy, J. Chem. Phys. 99 (1993) 2175.
[6] R. Trivedi, W. Kurz, Int. Mater. Rev. 39 (1994) 49.
[7] T. Kraft, H.E. Exner, Mater. Sci. Eng. A 173 (1993) 149.
[8] G.J. Merchant, S.H. Davis, Acta Metall. Mater. 38 (1990) 2683.
[9] P. Galenko, Phys. Lett. A 190 (1994) 292.
[10] R. Willnecker, D.M. Herlach, B. Feuerbacher, Appl. Phys. Lett. 56 (1990) 324.
[11] H.M. Twancy, J. Mater. Sci. 16 (1981) 2883.
[12] M. Raghavan, B.J. Berkowitz, J.C. Scanlon, Metall. Trans. 13A (1982) 979.
[13] H.M. Twancy, R.B. Herchenroeder, A.I. Asphani, J. Metals 35 (1983) 37.
[14] J.I. Akhter, M.A. Shaikh, M. Ahmad, M. Iqbal, K.A. Shoaib, W. Ahmad, J. Mater. Sci. Lett. 20 (2001) 333.
[15] H. Dong, X.Y. Li, T. Bell, J. Alloys Compd. 283 (1999) 231.
[16] A. Bruckner, E.K. Tschegg, A. Schuler, J. Mater. Sci. 25 (1990) 5220.
[17] H.M. Flower, P.B. Swann, D.R.F. West, Metall. Trans. 2 (1971) 3289.